33rd Annual International Conference of the IEEE EMBS
Boston, Massachusetts USA, August 30 - September 3, 2011

Objective Measure of Upper Extremity Motor Impairment in Parkinson's Disease with Inertial Sensors

Jeffrey D. Hoffman and James McNames

Abstract— **Functional motor impairment caused by Parkinson's disease and other movement disorders is currently measured with rating scales such as the Unified Parkinson's Disease Rating Scale (UPDRS). These are typically comprised of a series of simple tasks that are visually scored by a trained rater. We developed a method to objectively quantify three upper extremity motor tasks directly with a wearable inertial sensor. Specifically, we used triaxial gyroscopes and adaptive filters to quantify how predictable and regular the signals were. We found that simply using the normalized mean squared error (NMSE) as a test statistic permitted us to distinguish between subjects with and without Parkinson's disease who were matched for age, height, and weight. A forward linear predictor based on the Kalman filter was able to attain areas under the curve (AUC) in receiver operator characteristic (ROC) curves in the range of 0.76 to 0.83. Further studies and development are warranted. This technology has the potential to more accurately measure the motor signs of Parkinson's disease. This may reduce statistical bias and variability of rating scales, which could lead to trials with fewer subjects, less cost, and shorter duration.**

I. Introduction

THE Unified Parkinson's Disease Rating Scale (UPDRS) was first proposed in 1987 [1] to assess and track the severity of Parkinson's Disease (PD). It has since undergone revisions recommended by the Movement Disorder Society Task Force in 2003 [2]. The UPDRS consists of four sections: (1) mentation, behavior and mood; (2) activities of daily living; (3) motor; (4) complications [3]. These rating scales rely on the subjective judgment of a rater to visually assess the impairment during prescribed activities that comprise the motor section of the UPDRS. We examined the possibility of directly measuring impairment with an inertial sensor during two of these tasks: finger tapping and hand pronation-supination. This could ultimately obviate the rater and thereby reduce bias and variability of this instrument for measuring functional motor impairment in PD.

Recent advances in microelectromechanical systems (MEMS) have yielded gyroscopes and accelerometers fabricated on integrated circuit (IC) chips. Wearable instrumentation based on these sensors is capable of measuring motion in 3-space and are now commercially available from a variety of companies.

Recent research on the use of accelerometers and gyroscopes to assess tremor have shown good correlation with raters on the UPDRS tasks [4][5][6][7]. We propose to extend this technology from tremor to other types of motor impairment by using an inertial sensor to record motion during finger tapping (UPDRS part 3.4) and hand pronation-supination (UPDRS part 3.6).

In the UPDRS, halts, hesitations, slowing repetition rate, and decreasing displacement amplitude warrant higher (worse) scores [3]. The adaptation rate of filters based on least-mean squares (LMS), recursive least squares (RLS), and Kalman filter algorithms can be constrained by use of a parameter in the filter equations. By tuning the adaptation rate of the filter, one can constrain the filter such that regular, predictable signals produced by people without Parkinson's disease are closely tracked and less consistent signals produced by people with Parkinson's disease tracked less accurately. We used normalized mean squared error (NMSE) between the actual and predicted signals as a measure of the predictability and regularity of the signal. We hypothesized that this would correspond to the degree of motor impairment.

II. Methodology

A. Experiment Design

We used a wearable inertial sensor to record linear acceleration and angular velocity from 11 PD subjects and 35 controls performing parts 3.4 and 3.6 of the UPDRS. We used two variations on part 3.4: (1) pad-pad finger taping and (2) tip-knuckle finger tapping. We modified part 3.6 to increase exercise duration by allowing the subject to rest the upper arm at their side with bent elbow and producing a grip that simulates grasping a door knob. The accelerometer and gyroscope were attached at the second phalanx of the index finger with the *x*-axis lateral to the finger, the *y*-axis longitudinal with the finger, and the *z*-axis perpendicular to the finger nail.

This study was reviewed and approved by the institutional review board at Oregon Health & Science University.

The fully flexed form of the pad-pad finger tap is shown in Figure 1(a). The subject was instructed to repeatedly extend and flex the finger and thumb such that their orientation cycled from a 90 degree angle when fully extended to contacting the thumb and finger pads when fully flexed. The subject was instructed to cycle from full extension to full flexion as quickly as possible without

Jeffrey D. Hoffman and is a member of the Biomedical Signal Processing Laboratory and graduate student in the Department of Electrical and Computer Engineering at Portland State University, Portland, Oregon, USA. Email: jdhoffma@pdx.edu (corresponding author).

James McNames is director of the Biomedical Signal Processing Laboratory. He is also professor and chair of the Department of Electrical and Computer Engineering at Portland State University, Portland, Oregon, USA. Email: mcnames@pdx.edu.

compromising range of motion.

The fully flexed form of the tip-knuckle finger tap is shown in Figure 1(b). The instructions were the same as for the pad-pad finger tap except that the fully flexed form has finger tip contacting the knuckle of the thumb.

The fully clockwise form of the hand pronation-supination is shown in Figure 1(c). The subject was instructed to alternately rotate the hand fully clockwise then fully counter-clockwise. As in the previous exercises, the subject was instructed to cycle as quickly as possible without compromising range of motion.

The target duration for all exercises was 15 seconds. The subjects were asked to inform us of any pain, discomfort, or fatigue immediately so that we could terminate the trial. The tasks were performed in the sequence (1) pad-pad finger tap, (2) hand pronation-supination, and (3) tip-knuckle finger tap. The entire sequence was repeated twice on one side then twice on the other. Signals from the inertial sensor were collected and stored during all exercises lasting 10 seconds or more.

(a) Pad-pad finger tap (b) Tip-knuckle finger tap

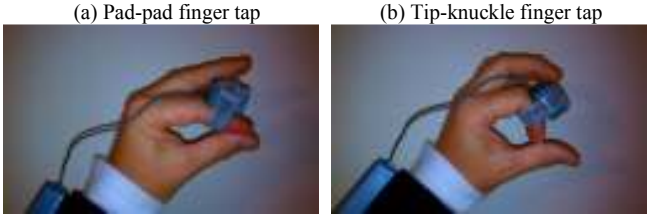

(c) Hand pronation-supination

Figure 1. Forms of UPDRS motor exam exercises

A. Instrumentation

Instrumentation consisted of a KinetiSense™ Biokinetic Analysis System [4] with software version 3.0 running on a Windows XP laptop. The KinetiSense™ system included finger mounted triaxial accelerometers and gyroscopes sampled at a rate of 128 Hz and transmitted wirelessly to a laptop via a wrist mounted BlueTooth® transceiver. Data collected on the laptop was stored in comma separated values (CSV) files for later processing using MATLAB® Student version R2010a.

B. Signal Processing

Predictability was quantified by the normalized mean squared error (NMSE) between a target signal and its forward linear prediction (FLP). The ideal FLP signal is deterministic, periodic, and close to sinusoidal. Of the inertial sensor signals recorded, angular velocity best fits those characteristics. For finger tapping, the axis of rotation is the x-axis, and we used $\omega = \omega_X$. For hand pronation-supination, the axis of rotation is somewhere in the *yz*-plane, and we used

$$\omega = \begin{cases} \text{sgn}(\omega_Y)\sqrt{\omega_Y^2 + \omega_Z^2}, & \Omega_Y > \Omega_Z \\ \text{sgn}(\omega_Z)\sqrt{\omega_Y^2 + \omega_Z^2}, & \Omega_Y \leq \Omega_Z \end{cases} \quad (1)$$

where

$$\Omega_Y = \sum \omega_Y^2, \ \Omega_Z = \sum \omega_Z^2 \quad (2)$$

A high level block diagram of the FLP is shown in Figure 2. The filtering operation predicts the future value $\omega(n+1)$ from current and past values as an inner product of a vector of coefficients **c** with the past and present values of discrete time sampled signal **ω**,

$$\hat{\omega}(n+1) = [\omega(n)\ \omega(n-1)\ \ldots \omega(n-M)]\mathbf{c} \quad (3)$$

where the $M\times1$ coefficient vector **c** is adapted to minimize the mean square error. We compute NMSE as the squared norm of the error signal **e** divided by the squared norm of the velocity signal **ω**.

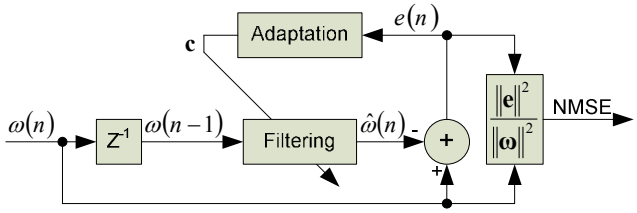

Figure 2. Block diagram of the one-step ahead FLP

We examined the performance of four different adaptive filtering algorithms: (1) Ordinary Least Squares (LS), (2) Least Mean Square (LMS), (3) Recursive Least Squares (RLS), and (4) Kalman Filter. We optimized each filter by repeating the NMSE computation over a range of model order and adaptation parameter specific to each filter. We then statistically analyzed the computed NMSE surfaces across subjects as described in section C below choosing the parameters that maximized area under the receiver operating characteristic curve (AUC). Details regarding the use of each filter are described in the following sections.

1) Least Squares Forward Linear Prediction (LSFLP)

The LSFLP was adapted from Manolakis [8] pages 411-413. The coefficient vector **c** is adapted after an *L* sample training interval at the beginning of the signal. The solution of the normal equations gives the value of **c** that minimizes squared error. We repeated NMSE computation varying model order *M* and training length *L* over the ranges $8 \leq M \leq 128$ and $256 \leq L \leq 512$ respectively.

2) Least Mean Squares Forward Linear Prediction (LMSFLP)

The LMSFLP was adapted from Widrow [9]. Unlike the LSFLP, the coefficient vector **c** is continuously adapted over

the entire length of the signal. A 144 sample training interval at the beginning of the signal was excluded from NMSE computation providing time for filter coefficients to settle. We repeated NMSE computation varying model order M and adaptation gain μ over the ranges $24 \leq M \leq 144$ and $0.1 \leq \mu \leq 1.9$ respectively.

3) Recursive Least Squares Forward Linear Predictor (RLSFLP)

The RLSFLP was adapted from Manolakis [8] pages 548-573. Like the LMSFLP, the coefficient vector **c** is continuously adapted over the entire length of the signal. A 256 sample training interval at the beginning of the signal was excluded from NMSE computation providing time for filter coefficients to settle. We repeated NMSE computation varying model order M and forgetting factor λ over the ranges $24 \leq M \leq 144$ and $0.9049 \leq \lambda \leq 0.9999$ respectively.

4) Kalman Forward linear Prediction (KFLP)

The KFLP was adapted from Kalman [10]. Like LMSFLP and RLSFLP, the coefficient vector **c** is continuously adapted over the entire length of the signal. A 512 sample training interval at the beginning of the signal was excluded from NMSE computation providing time for filter coefficients to settle. We varied model order M and processes variance q over the ranges $24 \leq M \leq 152$ and $1e\text{-}6 \leq q \leq 2e\text{-}5$ respectively.

C. Statistical Analysis

We quantified the ability of the algorithms to distinguish between people with and without Parkinson's disease using a lower-tailed student t-test with unequal variance and receiver operating characteristic (ROC) curves, which are used extensively in medical research [11]. ROC curves plot the probability of a true positive versus the probability of a false positive over a range of threshold values. If the subject's measured NMSE is less than the threshold NMSE, it is a negative test result. Otherwise, it is a positive test result. A positive test result for a person without PD is considered a false positive whereas a positive test result for a person with PD is considered a true positive. The null hypothesis is rejected in favor of the alternative when the p-value is less than our level of significance (0.05) and the area under the ROC curve (AUC) is large.

III. Results

The control subject population consisted of 17 females and 18 males ranging in age from 39 to 91 years, in weight from 92 to 280 pounds, and in height from 62 to 76 inches. The PD subject population consisted of 3 females and 8 males ranging in age from 59 to 75 years, in weight from 121 to 230 pounds, and in height from 62 to 73 inches. All PD subjects were off medication and had total clinician rated UPDRS motor exam scores ranging from 23 to 45 with an average of 32.05 and standard deviation of 6.15. The UPDRS finger tap scores ranged from 1.0 to 3.5 with an average of 2.25 standard deviation of 0.84. UPDRS hand pronation-supination scores ranged from 0 to 3.5 with an average of 1.7 and standard deviation of 0.88.

For PD subjects, each of the three exercises was performed 4 times (twice per side) during a single session. For controls, the number of trials varied depending on subject availability with one control performing the pad-pad finger tap 42 times (21 times per side) during 13 different sessions. In all cases and for each metric, all trials taken by a particular subject performing a particular exercise were averaged.

A comparison of angular velocity signals from a PD subject and control recorded during hand pronation-supination is shown in Figure 3. The PD signal is visibly less deterministic than the control signal.

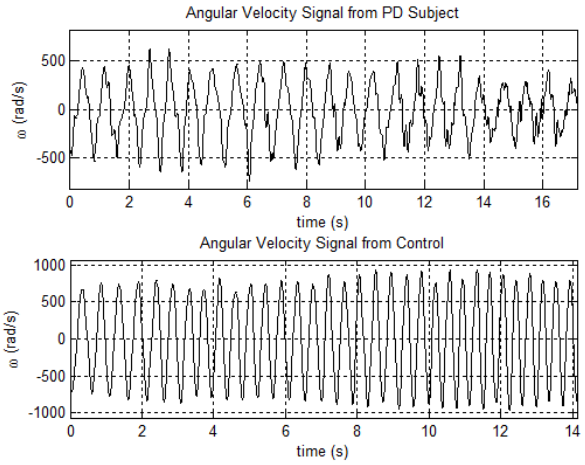

Figure 3. Comparison of angular velocity signals from a PD subject (top) and control (bottom). PD signals are less deterministic than controls.

We tuned adaptation and model order parameters for each FLP and exercise to yield peak AUC. By way of example, a plot of the AUC surface vs. forgetting factor λ and model order M calculated on the NMSE in RLSFLP during hand pronation-supination is shown in Figure 4. A peak at (λ, M) = (0.93, 104) is evident. Similar surfaces were used to tune the other filters for each exercise.

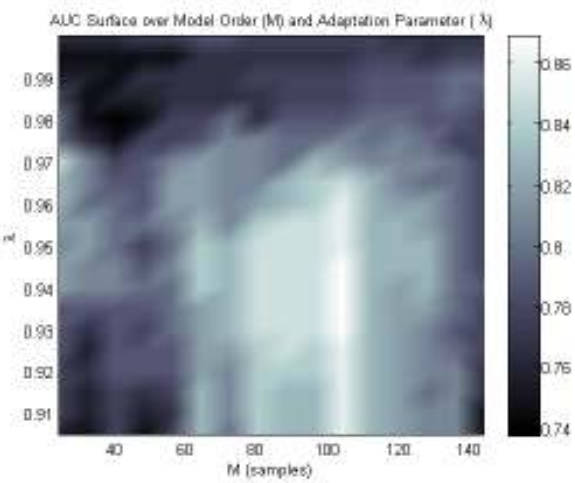

Figure 4. Plot of AUC surface vs. forgetting factor λ and model order M calculated on the NMSE in RLSFLP during hand pronation-supination.

Statistical analysis of the results showed that

discrimination was improved when the control group was reduced to those within age, height and weight limits of the PD subject group. Furthermore, discrimination was best on the dominant hand. Final p-value and AUC results using optimally tuned FLPs are listed in Table I.

TABLE I. AUC AND P-VALUE BY EXERCISE AND ALGORITHM

Algorithm	Pad-Pad Finger Tap		Tip-Knuckle Finger Tap		Hand Pronate-Supinate	
	AUC	P-val.	AUC	P-val.	AUC	P-val.
LS	0.503	0.639	0.677	0.301	0.818	0.134
LMS	0.749	0.042	0.828	0.009	0.808	0.076
RLS	0.487	0.710	0.697	0.182	0.869	0.036
Kalman	0.781	0.026	0.828	0.018	0.758	0.079

Clearly, LSFLP and RLSFLP did not perform well in either finger tap exercise. Examination of the LSFLP and RLSFLP histograms revealed a positive skew for both controls and PD subjects that did not exist in LMSFLP and Kalman FLP. Examination of the actual versus predicted signals collected from subjects in the skewed end of the histograms showed that LSFLP and RLSFLP exhibit significantly larger ripple in their impulse response than do LMSFLP and Kalman FLP. An example of this effect is shown in Figure 5. The sharp negative peaks of the finger tap signal produce ripple in LSFLP and RLSFLP response, while no ripple is evident in the LMSFLP and Kalman FLP. These sharp peaks are independent of PD and the resulting ripple dominates the error.

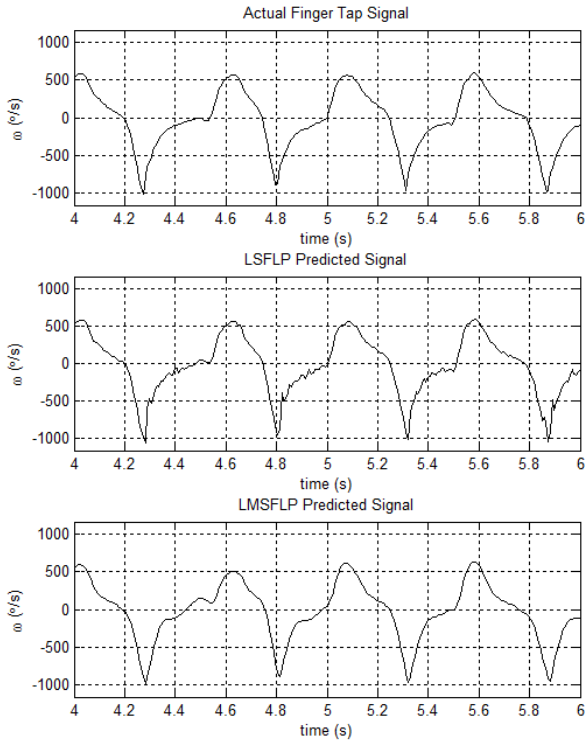

Figure 5. Plot of actual finger tap signal vs. LSFLP and LMSFLP predictions showing ripple in the impulse response of the LSFLP prediction.

IV. CONCLUSION

Comparing FLP algorithms, LMS and Kalman yielded high AUC and low p-value for all exercises. LS and RLS did not perform well for finger tapping due to ripple in their impulse response. Comparing exercises, tip-knuckle finger tapping produced best results with LMS and Kalman FLP. However, hand pronation-supination produced high AUC with all FLP algorithms.

As a general rule, LMS performed best with small adaption gain, RLS performed best with long memory, and Kalman with low process variance. Also, results showed a dependence on age, weight and height. This correlation needs to be quantified in order to compensate for these variables.

In conclusion, this research indicates that inertial sensors are a promising means of quantifying motor impairment in people with PD. The angular velocity signal collected from PD subjects performing finger tapping and hand pronation-supination exercises was less predictable than those collected from age, weight and height-matched controls. Other measures of regularity based on complex system analysis such as approximate entropy or traditional measures such as spectral flatness may also be helpful in this application. Further research and development is warranted.

REFERENCES

[1] S Fahn, RL Elton, UPDRS program members, "Unified Parkinsons Disease Rating Scale," *Recent Developments in Parkinsons Disease*, Macmillan Healthcare Information, Florham Park, NJ, vol. 2, pp. 153–163, 1987.

[2] CG Goetz, Movement Disorder Society Task Force on Rating Scales for Parkinson's Disease, "The Unified Parkinson's Disease Rating Scale (UPDRS): Status and recommendations," *Movement Disorders*, Movement Disorder Society, vol. 18, no. 7, pp. 738–750, 2003

[3] Movement Disorder Society Task ForceTask Force for Rating Scales in Parkinson's Disease, "Rating scales," The Movement Disorder Society, [Online] November 26, 2010 [Cited: November 26, 2010], http://www.movementdisorders.org/publications/rating_scales/.

[4] JP Giuffrida, DE Riley, BN Maddux, and DA Heldman, "Clinically deployable Kinesia technology for automated tremor assessment," *Movement Disorders*, New York, vol. 24, no. 5, pp. 723-730, 2009.

[5] A Salarian, H Russmann, C Wider, PR Burkhard, FJG Vingerhoets, K Aminian, "Quantification of tremor and bradykinesia in Parkinson's disease using a novel ambulatory monitoring system," *Biomedical Engineering, IEEE Transactions on* , vol. 54, no. 2, pp. 313-322, Feb. 2007

[6] JI Hoff, AA Plas, EAH Wagemans, and JJ Hilten, "Accelerometric assessment of levodopa-induced dyskinesias in Parkinson's disease," *Movement Disorders*, vol. 16, no. 1, pp. 58-61, Jan. 2001.

[7] EJW Van Someren, BFM Vonk, WA Thijssen, JD Speelman, PR Schuurman, M Mirmiran, DF Swaab, "A new actigraph for long-term registration of the duration and intensity of tremor and movement," *Biomedical Engineering, IEEE Transactions on* , vol. 45, no. 3, pp. 386-395, March 1998.

[8] DG Manolakis, VK Ingle, SM Kogan, *Statistical and Adaptive Signal Processing*, Norwood MA, Artec House, 2005.

[9] B. Widrow and M.E. Hoff, Jr., "Adaptive Switching Circuits," *IRE WESCON Convention Record*, vol. 4, pp. 96-104, August 1960.

[10] RE Kalman, "A new approach to linear filtering and prediction problems," *Transaction of the ASME – Journal of Basic Engineering*, vol. 82, pp. 35-45, 1960.

[11] T Fawcett, "An introduction to ROC analysis," *Pattern Recognition Letters*, vol. 27, no. 8, pp. 861-874, 2006.